



Investigating the effectiveness of fluid viscous damper in reducing the effect of seismic sequence on steel bending frame designed on type c soil

Javad Pourali ^{a*}

^a*School of Civil Engineering, Higher Education Institute of Tabari, Babol, Iran*

Journals-Researchers use only: Received date: 2023.02.20; revised date: 2023.03.15; accepted date: 2023.03.20

Abstract

Aftershocks can always cause the collapse of structures damaged by the main earthquake. In this article, the seismic performance of an 8-story steel bending frame designed in c-type soil was first subjected to the seismic sequence of an earthquake and an aftershock, and then the same building with the addition of a fluid viscous damper (Fluid Viscous Damper) was evaluated. The results showed that the seismic performance of the studied frame under the effect of severe aftershocks with the presence of a liquid viscous damper is very different from the case without FVD. For example, the maximum displacement of the structural floors was reduced by 60% compared to the case without a damper. It was also found that while most of the aftershocks in buildings without dampers cause a significant increase in the permanent displacement of the roof, in the presence of dampers, this amount has decreased significantly, although in general, the damage caused by the effect of aftershocks on the building is much more as it will be from a state in which the structure is only subjected to the main earthquake © 2017 Journals-Researchers. All rights reserved. (DOI: <https://doi.org/10.52547/JCER.5.2.46>)

Keywords: Aftershock, Mainshock; Seismic sequence; Steel moment frame; Fluid Viscous Damper

1. Introduction

The earthquake is a natural phenomenon that has repeatedly horrified man in human history and has destroyed many cities and villages along with severe human and financial casualties. Historical evidence has shown that large earthquakes are often followed by repeated aftershocks and form a sequence of

earthquakes and aftershocks. Strong aftershocks can increase the level of damage to structures with new damage and may also cause weakening or collapse of structures that were previously damaged under the main earthquake.)But, due to the short time between the occurrence of the aftershock and the main earthquake, they have not been repaired yet([1]. An example of this is the main earthquake in Chile on February 27, 2010 ($M_w = 8.8$), which caused severe

* Corresponding author. Tel.: +98-9116189500; e-mail: j.pourali66@gmail.com.

damage to the southern and central regions of Chile with 360 aftershocks with a magnitude of more than 5 between February 27 and April 26. Among these aftershocks were 21 magnitudes greater than 6 [10]. The first analytical study on the nonlinear behavior of single-degree-of-freedom (SDOF) systems exposed to the time-history records of the 1972 Managua Post-Earthquake was conducted by Mahin (1980). He observed that displacement demand ductility (the ratio of maximum inelastic displacement to system yield displacement) in elastoplastic SDOF systems at the end of the main aftershock increases slightly relative to the original earthquake. Mahin examined the effects of this sequence on structures by setting two records of major earthquake and aftershock. This had one major drawback; it did not take into account the effects of the system's free vibration on the distance between the main earthquake and the aftershock. In subsequent studies, a time interval between the main earthquake and the aftershock was considered and it was assumed that at this distance the system would stop moving. Later, some other researchers used a distance of 20 to 100 seconds in their research depending on the type of structures [4,5]. In fact, this time interval is considered only to end the free vibration time of the system, which by examining the behavior of the structures studied in this study, 40 seconds was found to be a suitable number. Figure 1 shows a schematic of how earthquake and aftershock acceleration maps are placed one after the other.

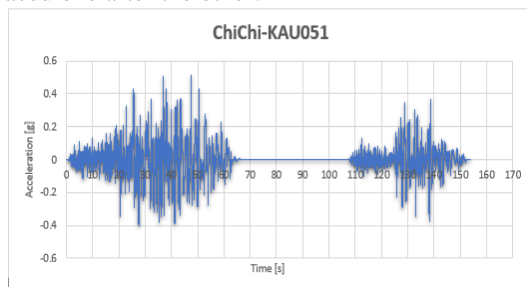


Figure 1. How to place the acceleration of earthquake and aftershock

Garcia (2012) examined the characteristics of a wide range of earthquakes and corresponding aftershocks on the seismic response of buildings and showed that the dominant period, as well as the duration of the main earthquake and aftershocks, were

statistically weakly correlated. Therefore, the production of artificial seismic sequences from the main earthquake as a basis for the production of aftershocks, even with a smaller amplitude, does not make sense because the frequency and duration of the earthquake are completely different [9]. Therefore, it can be said that it is necessary to use real data to evaluate the performance of existing structures under seismic sequences. Abdollahzadeh et al. (2017) with the help of real seismic sequences and by examining the energy distribution in buildings designed by conventional elastic methods as well as modern plastic design methods based on performance, found that aftershocks have a destructive effect on floors that suffer more damage under the main earthquake. Have seen will have [9]. Recently, several researches have been conducted in the field of seismic evaluation of structures under seismic sequences, in all of which the effect of aftershock in increasing the vulnerability of the structure has been confirmed [10,11]. However, design codes still do not explicitly consider the effects of aftershocks and the cumulative damage caused by them in the design of earthquake-resistant structures. The reason for this is probably due to the many uncertainties in the capacity of structures damaged after the main earthquake, the complexity of aftershock characteristics and the probability of their occurrence and the general lack of system fragility models to evaluate the performance of structures [2, 12].

2. Modeling

To evaluate the vulnerability of MDOF structures (several degrees of freedom) under the effect of earthquake and aftershock sequence, an 8-story building in Tehran of medium steel bending frame type in types (C) of soil based on LRFD method Article 10 of the National Building Code and the fourth edition of Standard 2800 [6] were designed. These structures have three openings of 5 meters in each direction and the height of the floors is 3.2 and the height of the parking lot is 2.7. First, the design of this building was done according to the residential use and located on a relatively high-risk area according to the definition of 2800 standard with the help of ETABS software. Then, for two-dimensional analysis

of the critical frame, the selection and seismic performance of this frame were evaluated using time history analyzes by applying natural earthquake and

aftershock records using OpenSees finite element software. Figure 3 shows the three-dimensional and two-dimensional views of the designed frame.

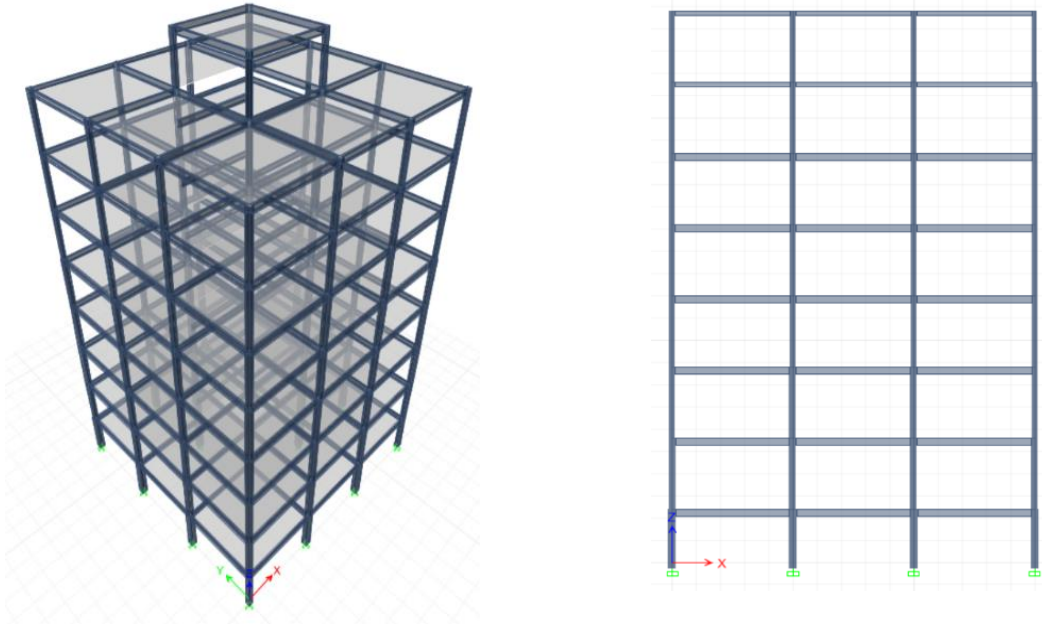


Figure 2 and 3. Three-dimensional and two-dimensional view of the designed frame

In the definition of steel, non-linear materials (steel02) in the OpenSees material library were used and the cross-section of the members was made of fiber. This command separates the cross section into smaller areas and summarizes the stress-strain response of the materials for these areas to obtain the resultant behavior. Tables 1 and 2 provide a list of sections designed in the critical frame.

Table 1

List of designed section (Type C soil)

Columns	Beams
BOX180X8	PG-W180X6-F150X8
BOX200X8	PG-W180X6-F150X15
BOX200X10	PG-W300X6-F150X10
BOX200X12	PG-W300X6-F150X12
BOX240X10	PG-W300X6-F150X15
BOX240X12	PG-W300X6-F150X20
BOX240X15	
BOX240X20	
BOX300X20	
BOX180X8	

2.1. Fluid viscous damper

Fluid Viscous Damper systems are hydraulic equipment that is used to dissipate kinetic energy caused by seismic vibrations or to deal with impacts between structures. These equipments are diverse and can be designed in such a way that they absorb the desired load (for example, earthquake and wind loads), but allow the structure to move freely against other conditions such as heat-induced movements. FVD typically consist of a piston head with orifices contained in a cylinder filled with a highly viscous fluid, usually a compound of silicone or a similar type of oil. Energy is dissipated in the damper by fluid orifice when the piston head moves through the fluid. The fluid in the cylinder is nearly incompressible, and when the damper is subjected to a compressive force, the fluid volume inside the cylinder is decreased as a result of the piston rod area movement. A decrease in volume results in a restoring force. This undesirable force is prevented by using an accumulator. An

accumulator works by collecting the volume of fluid that is displaced by the piston rod and storing it in the makeup area. As the rod retreats, a vacuum that has been created will draw the fluid out. A damper with an accumulator is illustrated in Fig. 4[7].

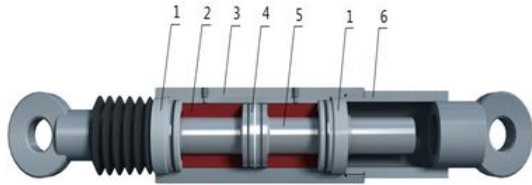


Figure 4. Fluid viscous dampers (FVD).

1-end cover; 2-damping medium; 3-cylinder block; 4-piston; 5-piston rod; 6-connector

2.1.1. Characteristics of fluid viscous dampers

FVD are characterised by a resistance force F . It depends on the velocity of movement, the fluid viscosity and the orifices size of the piston. The value of P is given by the relationship.

$$P = C_d (\dot{U}d)^\alpha \sin(\dot{U}d)$$

with

$$U_d(t) = U_0 \sin(\omega \cdot t)$$

Where

$U \cdot d$ is the velocity between two ends of the damper;

C_d is the damping constant;

U_0 is the amplitude of the displacement,

ω is the loading frequency, and t is time;

α is an exponent which depends on the viscosity properties of the fluid and the piston.

The value of the constant α may be less than or equal to 1. Figs. 5 and 6 show the force velocity and the force displacement relationships for three different types of FVD. They characterise the behaviour of the viscous damper. With $\alpha = 1$ the device is called linear viscous damper and for $\alpha < 1$ non-linear FVD which is effective in minimising high velocity shocks. Damper with $\alpha > 1$ has not been seen often in practical application. The non-linear damper can give a larger damping force than the two other types (Fig. 5).

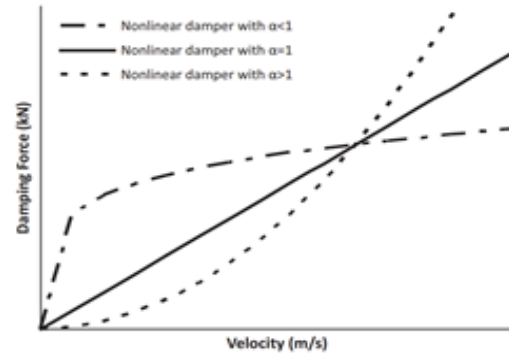


Figure 5. Force velocity relationship of FVD.

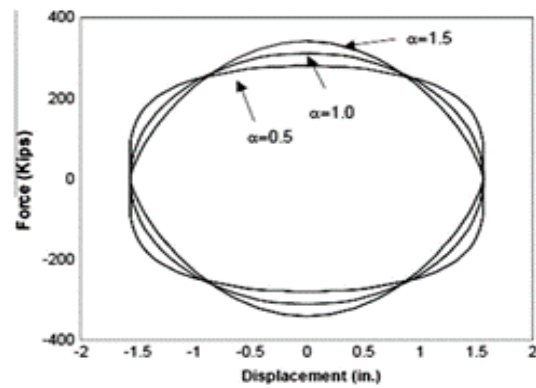


Figure 6. Force displacement relationship of FVD.

Fig. 6 shows that the plot has different shapes for the different values of α . At the frequency of loading used to create the loops enclosed areas for the different damper are all equal, but the values of the damping coefficient are all different. The resisting force in the FVD, P , can be described by the following equation:

$$P = K_1 U_d + C_d \frac{dU_d}{dt}$$

Where

K_1 is the storage stiffness and C is the damping coefficient given by

$$C_d = \frac{K_2}{\omega}$$

Where

K_2 is the loss stiffness [7]. In the table below, the design specifications of several types of FVD are presented. In this study, the 500 kN model was used.

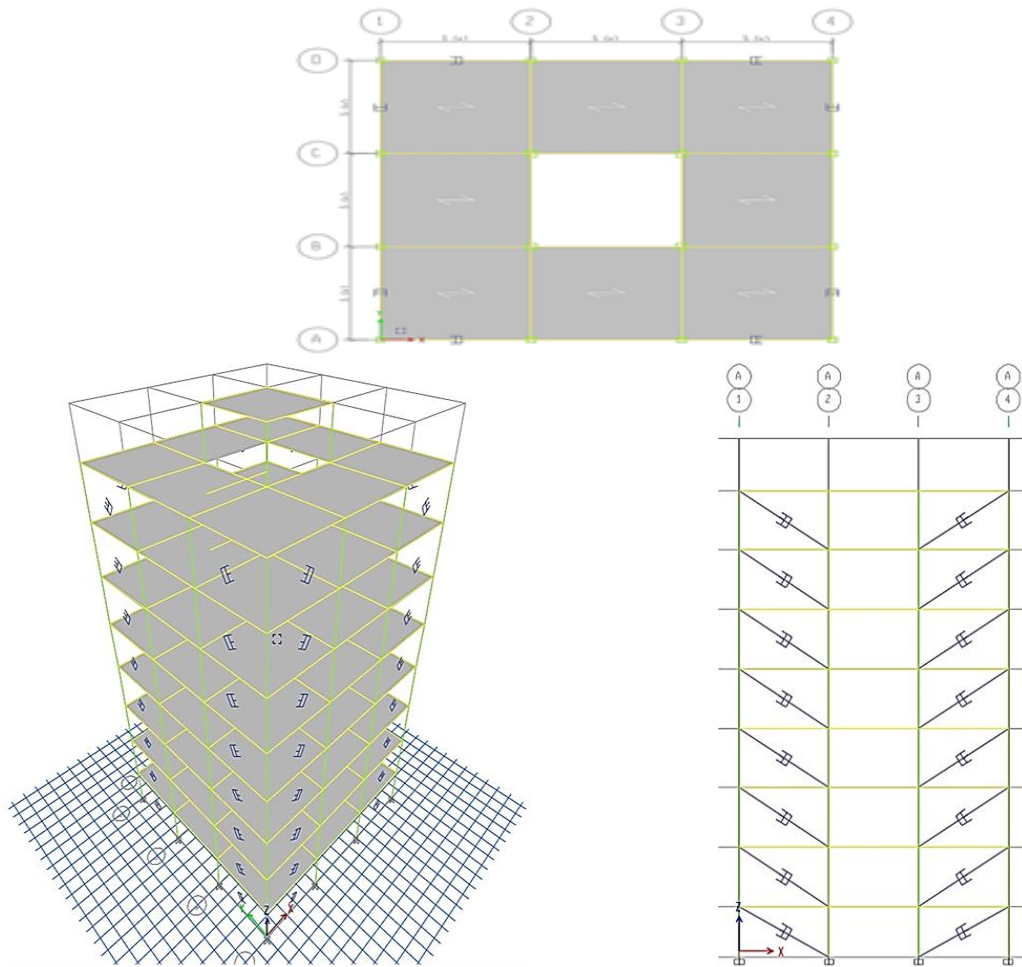


Figure 7. Three-dimensional, plan and two-dimensional view of the designed frame white FVD.

Table 3

FVD with different capacity force (kN)

Force (kN)	Taylor devices model number	Spherical bearing bore Diameter (mm)	Mid-stroke length (mm)	Stroke (mm)	Clevis Thickness (mm)	Maximum clevis width (mm)	Clevis depth (mm)	Bearing thickness (mm)	Maximum cylinder diameter (mm)	Weight (kg)
250	17120	38.10	787	±75	43	100	83	33	114	44
500	17130	50.80	997	±100	55	127	102	44	150	98
750	17140	57.15	1016	±100	59	155	129	50	184	168
1000	17150	69.85	1048	±100	71	185	150	61	210	254

Past studies have shown that records must be scaled to the desired hazard level to achieve proper seismic behavior [3]. In this study, 12 raw accelerometers were extracted from PEER site data in accordance with the

soil type and were compared and scaled according to the instructions of the fourth edition of the 2800 standard. Table 3 shows the characteristics of each of

the corresponding earthquake and aftershock accelerometers.

Table 3
Characteristics of earthquake and aftershock acceleration

Name of earthquake	Station	Magnitude of earthquake	magnitude of the aftershock	Shear wave velocity
HOLISTER	Holister	5.6	5.5	198
Imperial Valley	Holtville	6.53	5.01	202
Northwest	Jiashi	6.1	5.8	240

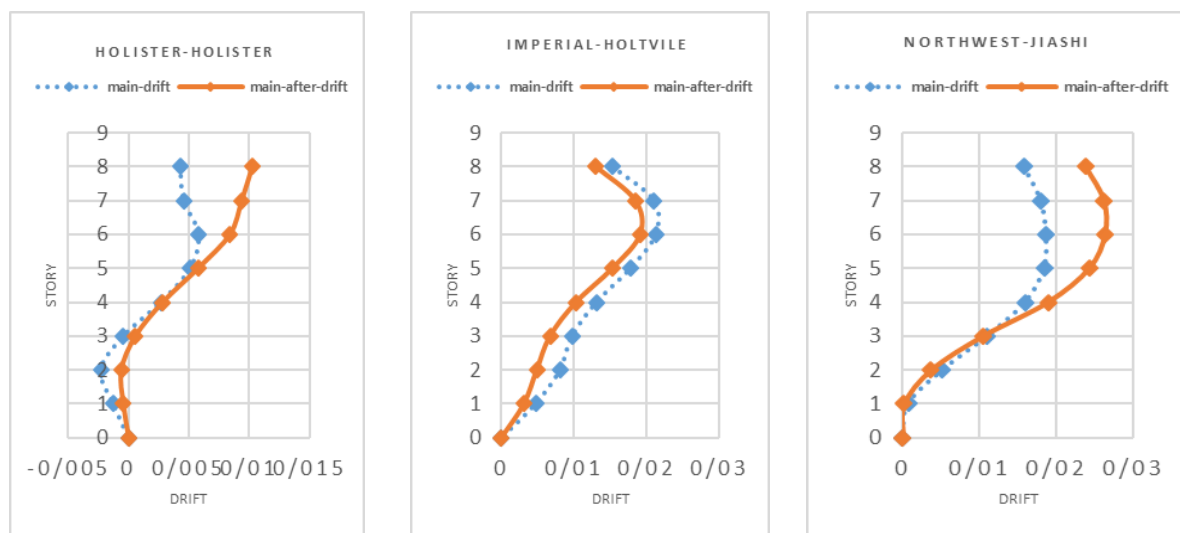
It should be noted that regarding the scale of aftershocks, the adaptation coefficient was used to maintain the PGA ratio of earthquake and aftershock. According to Table 4, the ratio of PGA aftershock to the main earthquake is:

Table 4
Ratio of PGA aftershock to main earthquake

Name of earthquake					
Northwest-Jiashi		Holister-Holister		Imperial-Holtville	
PGA after / PGA ma	0.873402	PGA after / PGA ma	-	PGA after / PGA ma	-
			0.61133		0.44463

3. Comparison of floor drift distribution

The frames are exposed to the seismic sequences of the accelerometers presented in Table 3 under time history analysis, and the drift changes of the classes in height are shown in Figures 1. As can be seen from the diagrams related to the drift of the floors, the aftershock in some cases leads to a strong increase in the drift of the structure, and in some cases, the aftershock did not have much effect on the main structure, which is justified due to the very small intensity of the aftershock in the earthquake. Therefore, the main damage occurs during the main earthquake. However, according to the 2800 standard guidelines, if these three records are selected for design, maximum results should be used. Therefore, it is observed that aftershocks can have very destructive effects (increasing displacement up to more than double) that ignoring these effects in the design process can have catastrophic consequences during an earthquake. Another issue that seems to be important is the change of drift direction. This change in drift direction may cause severe damage to the structure, and it is possible that the structure will not be able to withstand such a deformation during severe earthquakes.



Graphs 1. Type C soil drift change diagrams

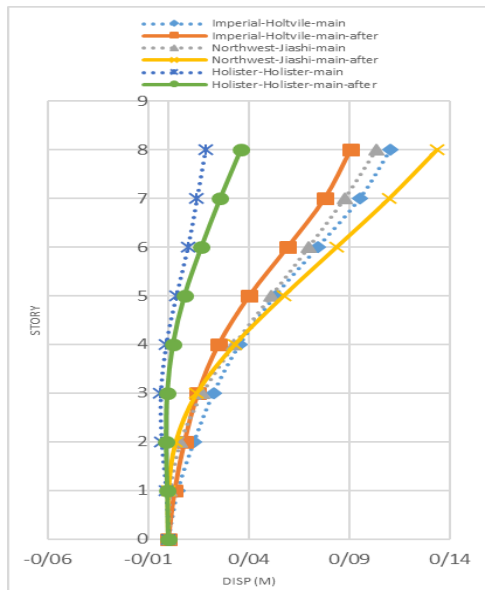


Figure 8. Permanent displacement diagrams whitout FVD.

4. Comparison of permanent displacement distribution of floors

Examining the drift distribution of floors at the collapse level of the damaged structure, it was found that with the increase of damage under the main earthquake, the distribution of damage is more concentrated in the same floors damaged in the main earthquake, while the same record in a healthy structure causes the failure of another floor. Comparison of permanent displacement distribution of floors. Finally, the remaining displacement of the elements in both healthy and damaged structures is investigated. The parameter of relative displacement, which is considered as a good representative for damage to structural members, also strongly depends on the type of damage caused by the main earthquake. The drift changes of the floors in the

Table 4

Ratio of displacement ratio of the structure under the effect of the seismic sequence in comparison with the main earthquake In type C soil								
Record name	floors							
	ST8	ST7	ST6	ST5	ST4	ST3	ST2	ST1
Imperial-Holtville	0.82	0.82	0.80	0.76	0.71	0.66	0.63	0.67
Northwest-Jiashi	1.29	1.25	1.20	1.12	1.01	0.85	0.65	0.19
Holister-Holister	1.94	1.81	1.70	2.09	-1.78	0.13	0.30	0.36

primary and damaged structures in different soil types are shown in Figures 8 to 12. As can be seen from Figures 8 to 12, the permanent displacement of the roof under the effect of seismic sequence is sometimes less than the permanent displacement of the roof under the effect of the main earthquake alone. This phenomenon expresses the important issue that aftershocks do not necessarily increase the permanent displacement of the structure. In examining the permanent displacement of the roof, it should be noted that the structure may not stop at its maximum permanent displacement due to successive earthquakes and as a result have less permanent displacement, although in this case, the damage to the structure has increased.

5. Conclusion

To evaluate the response of steel MDOF structures under the effects of seismic sequencing, an 8-story building with medium Steel moment system in types C of soil was designed according to version 4 of 2800 standard by LRFD method. Then the same building was designed with the addition of Fluid Viscous Damper (FVD) It was subjected to seismic sequence of earthquake and aftershock. Then, the most critical frame of each structure was selected for modeling in opensees software and finally, the performance of steel bending frames was investigated through applying natural records of an original earthquake and scaled aftershock according to standard criteria 2800 in terms of maximum relative –

Table 5

Direction	MAX Story displacement	
	EX	EY
Without FVD	265.93 mm	219.07mm
With FVD	74.371mm	73.625mm
Reduction rate%	%72	%66

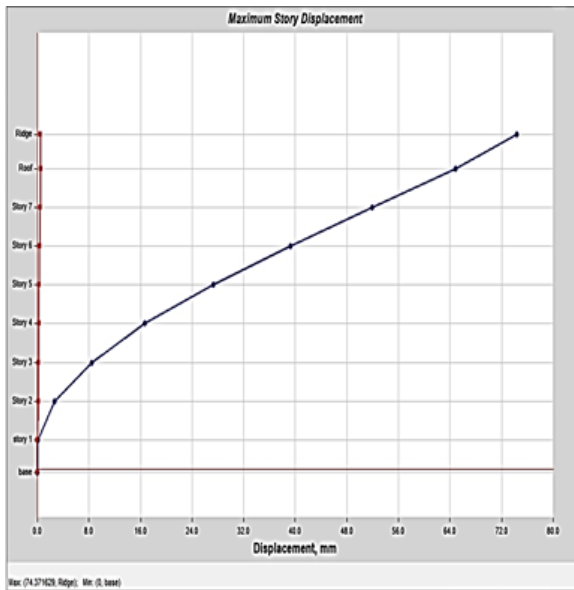


Figure 9. Max displacement whit FVD. -EX

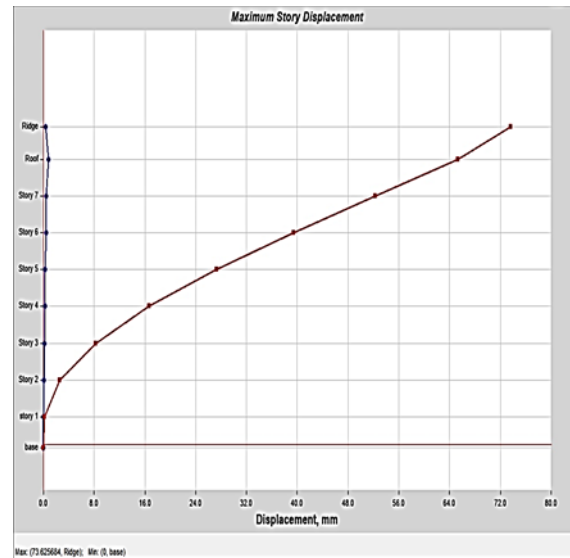


Figure 10. Max displacement whit FVD. -EY

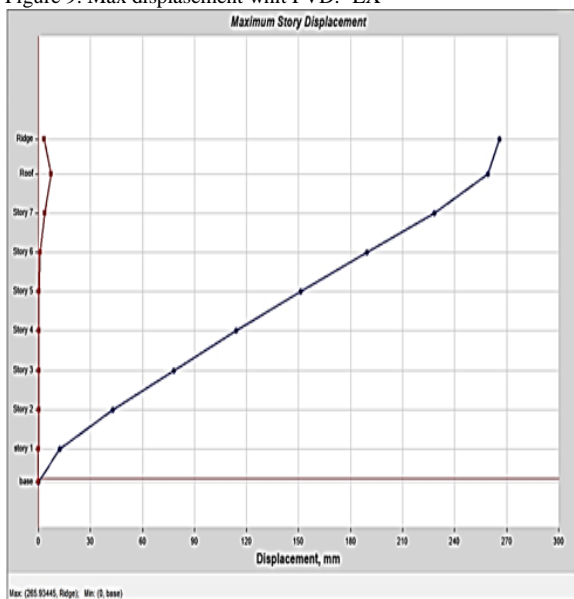


Figure 11. Max displacement whitout FVD. -EX

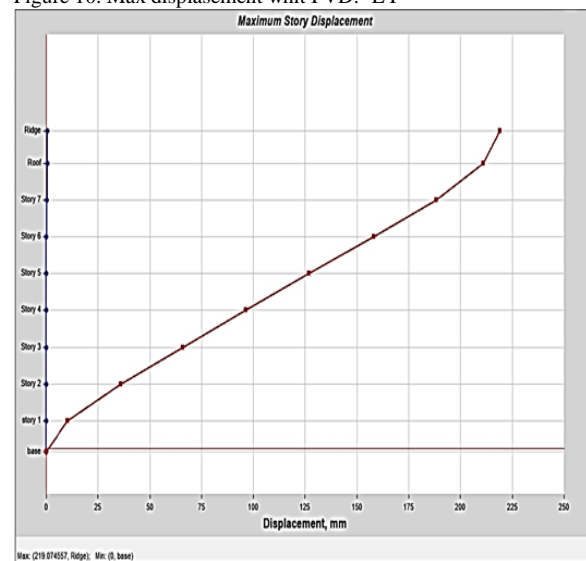


Figure 12. Max displacement whitout FVD. -EY

displacement within the floor and relatively lasting displacement which is considered as a good representative for structural organ damage and the following results were obtained.

1- The results showed that the seismic performance of the studied frame under the effect of severe aftershocks with the presence of a liquid viscous damper is very different from the case without FVD. For example, the maximum displacement of the structural floors was reduced by 60% compared to the

case without a damper. It was also found that while most of the aftershocks in buildings without dampers cause a significant increase in the permanent displacement of the roof, in the presence of dampers, this amount has decreased significantly, although in general, the damage caused by the effect of aftershocks on the building is much more as it will be from a state in which the structure is only subjected to the main earthquake.

2- Comparing the residual displacement of the elements in the two healthy and damaged structures, it was found that the residual displacement in the damaged structure is strongly dependent on the type of damage caused in the main earthquake. In fact, depending on the category of damage caused by the earthquake to the healthy structure, the focus of damage in the damaged structure has changed. This result can be seen due to the shape of the behavioral curves for structures with different percentages of damage. In some stimuli, there was no significant difference between the behavior of damaged and healthy structures.

3- By examining the drift distribution of floors in the collapse level of the damaged structure, it was found that with the increase of damage under the main earthquake, the distribution of damage is more concentrated in the same damaged floors in this earthquake, while the same record in a healthy structure causes damage in another floor.

References

- [1] G. yeo & A. Cornell S(2005)"stochastic Characterization and Decision Bases under Time-Dependent Aftershock Risk in Performance-Based Earthquake Engineering", PEER report.
- [2] Nazari. N, De Lindt.W, Li.Y,(2015)"Quantifying Changes in Structural Design Needed to Account for Aftershock Hazard", Journal of Structural Engineering.
- [3] Kiani, J. and Khanmohammadi M. (2015). New approach for selection of real input ground motion records for incremental dynamic analysis (IDA). Journal of Earthquake Engineering 19, no. 4: 592-623.
- [4] Mahin SA. (1980) Effects of duration and aftershocks on inelastic design earthquakes. In: Proceedings of the seventh world conference on earthquake engineering. vol. 5. p. 677-9.
- [5] Fragiocomo M, Amadio C, Macorini L. (2004) Seismic response of steel frames under repeated earthquake ground motions. Eng Struct;26:2021-35.
- [6] Earthquake Design Regulations, Standard 7, Edition 4, Building and Housing Research Center, Journal No. Z-1, First Edition 2014
- [7] A. Ras, N. Boumechra, Seismic energy dissipation study of linear fluid viscous dampers in steel structure design, Alexandria Eng. J. (2016),
- [8] Ruiz-Garcia J. Mainshock-aftershock ground motion features and their influence in building's seismic response. Journal of Earthquake Engineering 2012; 16(5):719-37.
- [9] Abdollahzadeh G.R., Mohammadgholipour A., Omranian E. (2017). Seismic evaluation of steel moment frames under mainshock-aftershock sequence designed by elastic design and PBPD methods Journal of Earthquake Engineering, (accepted).
- [10] Banon, H.,J.M.Biggs, and H.M.Irvine.."seismic Damage of Reinforced Concrete Frames." Journal of the structural Division,ASCE 107 (ST9) 1713-1729-1981
- [11] Hosseinpour F., and Abdelnaby A. E. (2017). Fragility curves for RC frames under multiple earthquakes. Soil Dynamics and Earthquake Engineering 98: 222-234.
- [12] Omranian E, Abdelnaby A. E., Abdollahzadeh Gh.R, Rostamian M., Hosseinpour F., Fragility Curve Development for the Seismic Vulnerability Assessment of Retrofitted RC Bridges under mainshock-aftershock seismic sequences, Structures Congress 2018 (accepted).
- [13] Abdelnaby, A. E.(2012)"Multiple earthquake effects on degrading reinforced concrete structures." Doctoral dissertation, Univ. of Illinois, Urbana-Champaign, IL.